Compliant Mechanisms: Implementation of Topological Optimization Method for the Development of Robotic Gripper with Flexible Finger

Brandon Lopez [1,*], Jaime Bakir [2], and Bernardo Quiroga [1]

[1] Departamento de Ciencias Exactas e Ingenierías, Universidad Católica Boliviana "San Pablo", Cochabamba, Bolivia
[2] Centro de Investigación en Ciencias Exactas e Ingenierías (CICEI), Universidad Católica Boliviana "San Pablo", Cochabamba, Bolivia
Email: lpzg.brandon@gmail.com (B.L.); jbakir@ucb.edu.bo (J.B.); ber.quiroga.turdera@gmail.com (B.Q.)
*Corresponding author

***Abstract*—This study presents the design, optimization, and experimental validation of low-cost, 3D-printed robotic grippers utilizing compliant mechanisms. The development is based on a three-dimensional Topology Optimization Method (TOM) implemented with the Solid Isotropic Material with Penalization (SIMP) approach. The Method of Moving Asymptotes (MMA) was employed to solve the associated nonlinear optimization problems for synthesizing flexible fingers, while a quadratic approximation method was utilized for designing rigid support structures. Two distinct objective functions were formulated: the first aimed to maximize the output displacement of a monolithic Polylactic Acid (PLA) finger by exploiting material compliance, and the second focused on minimizing the weight of the support structures under stiffness constraints. The optimized designs were fabricated via additive manufacturing and assembled into two-, three-, and four-finger gripper configurations. Experimental evaluation on an ABB IRB-120 robotic arm demonstrated the grippers' exceptional adaptability in manipulating objects of varied geometries and surface textures. Furthermore, payload capacity tests revealed maximum loads of 1.5 kg, 2.2 kg, and 2.7 kg for the two-, three-, and four-finger grippers, respectively. The results confirm that the proposed methodology, centered on MMA-based 3D topology optimization, provides an effective framework for developing high-performance, low-cost compliant robotic grippers.**

***Keywords*—compliant mechanism, gripper, topology optimization, Solid Isotropic Material with Penalization (SIMP), method of moving asymptotes, 3D printing, Finite Element Analysis (FEA)**

I. Introduction

The ability to grasp and manipulate objects with varying geometries and fragility is a fundamental requirement for advanced robotic systems. A central challenge in gripper design lies in achieving adaptive functionality: applying insufficient force may lead to object slippage, while excessive force can cause damage. Traditional solutions, which employ multiple rigid joints and actuators to increase degrees of freedom, often result in complex, costly, and heavy designs [1, 2]. To overcome these limitations, compliant mechanisms have emerged as a promising alternative. These monolithic structures utilize elastic deformation to generate motion, thereby reducing part count, assembly complexity, and weight while offering inherent robustness and backlash-free operation [1, 3].

The Topology Optimization Method (TOM) provides a systematic, computational approach for designing high-performance compliant mechanisms. It automates the distribution of material within a design domain to extremize a predefined objective function, such as maximizing output displacement, subject to constraints like volume reduction [2, 4]. While TOM has been widely adopted, its implementation domain—either in two or three dimensions—profoundly influences the outcome. Although 2D optimization reduces computational expense, it necessitates significant designer interpretation to construct a functional 3D model, potentially introducing inaccuracies [5]. In contrast, direct 3D topology optimization yields more efficient and manufacturable geometries, though it demands substantial computational resources and robust algorithms to solve the associated nonlinear equations [1, 6]. Despite its advantages, the application of 3D TOM for compliant mechanisms, particularly using advanced nonlinear solvers like the Method of Moving Asymptotes (MMA), remains less explored compared to 2D implementations or simpler optimization schemes.

This work reports on the implementation of a three-dimensional TOM for the development of robotic grippers with fully flexible fingers. The Solid Isotropic

Manuscript received July 14, 2025; revised August 22, 2025; accepted December 1, 2025; published March 27, 2026.

Material with Penalization (SIMP) method was employed to define the material distribution, while the MMA was implemented to solve the nonlinear optimization problem for the compliant fingers. A comparative analysis with a conventional quadratic approximation method underscores the superiority of the MMA in achieving convergence and generating efficient, functional designs. The optimized structures, alongside rigid supports also developed through TOM, were fabricated using Fused Deposition Modeling (FDM) with Polylactic Acid (PLA) filament. The resulting grippers, configured with two, three, and four fingers, were mounted on an ABB IRB-120 robotic arm, and their adaptability and payload capacity were rigorously validated experimentally.

This study aims to serve as a reference for the effective implementation of MMA in 3D structural optimization for compliant mechanisms. The article is structured as follows: Section II provides a comprehensive literature review. Section III details the methodology, encompassing the TOM theory, computational implementation, and the experimental setup. Section IV presents and discusses the results, and Section V summarizes the principal conclusions.

II. Literature Review

The development of robotic grippers capable of adaptive manipulation represents a significant focus within robotics research. This section reviews the foundational concepts, design methodologies, and manufacturing technologies relevant to compliant grippers, establishing the context and necessity for the present work.

A. Fundamentals and Evolution of Compliant Mechanisms

Compliant Mechanisms (CMs) generate motion through the elastic deformation of a monolithic structure, eliminating the need for traditional hinges, bearings, and assemblies. This paradigm offers profound advantages, including simplified fabrication, reduced part count, minimal backlash, and inherent potential for miniaturization [1, 3]. The field has evolved from intuitive, nature-inspired designs to a rigorous engineering discipline, thanks in large part to foundational work that systematized their analysis and synthesis [2, 7]. Early applications were often constrained to simple, planar structures due to analytical complexity. However, the convergence of computational power and sophisticated optimization algorithms has enabled the design of complex, high-degree-of-freedom CMs, making them increasingly viable for advanced applications such as precision manipulators and adaptive robotic grippers [5, 6].

B. Topology Optimization as a Design Tool for Compliant Systems

Topology Optimization (TOM) has emerged as the preeminent computational method for designing non-intuitive, high-performance CMs. Its core function is to algorithmically distribute material within a predefined design domain to extremize an objective function—such as maximizing output displacement or mechanical advantage—while satisfying constraints like volume reduction or stress limits [8]. The SIMP method is a cornerstone of modern TOM, facilitating this process by interpolating material properties between "solid" and "void" states and using a penalty factor to drive the solution toward a clear, manufacturable 0–1 density distribution [9, 10].

The choice of optimization algorithm is critical, particularly for the nonlinear problems inherent in CM design. While methods like Optimality Criteria (OC) are efficient for linear compliance minimization, the MMA, developed by Svanberg [11], has proven superior for handling the complex, nonlinear constraints required to generate efficient, path-generating compliant mechanisms [12, 13]. The implementation domain—2D versus 3D—further dictates the outcome. Many studies have successfully employed 2D TOM for its computational efficiency [14, 15]. However, as Liu and Tovar [16] argue, 2D results are inherently limited and require significant designer interpretation and manual "extrusion" to create a 3D model, a process that can compromise the optimized performance. In contrast, 3D TOM directly generates geometries that are readily manufacturable and mechanically coherent in three dimensions, providing a more direct and reliable design pathway, albeit at a higher computational cost [1, 17].

C. Additive Manufacturing and Material Considerations for Functional Grippers

The advent of Additive Manufacturing (AM) has been a key enabler for fabricating the complex, organic geometries generated by TOM. Fused Deposition Modeling (FDM) with PLA is particularly prevalent in research and prototyping due to its low cost, accessibility, and ease of use [15, 18]. However, the deployment of PLA in functional, load-bearing CMs presents specific challenges. Material science studies have highlighted PLA's inherent brittleness and poor fatigue resistance compared to more ductile polymers like Thermoplastic Polyurethane (TPU) [19, 20]. Its mechanical performance is also highly anisotropic, being dependent on print orientation and inter-layer adhesion strength—a critical factor that must be accounted for during the design and validation phases [21, 22].

Consequently, researchers have adopted various strategies to overcome these limitations. Some works combine PLA with flexible materials in multi-material prints or assemblies to enhance performance [7]. Others, like Sun *et al.* [1], bypass these limitations by using high-end AM technologies like Selective Laser Sintering (SLS) with advanced polymers, achieving remarkable payloads (8.3 kg) but at a significantly higher cost. This creates a clear trade-off: low-cost FDM/PLA is accessible but may limit performance, while high-performance SLS is often prohibitively expensive for widespread adoption. This dichotomy underscores the need for sophisticated design methodologies that can fully exploit the potential of low-cost materials and processes.

D. Critical Synthesis and Identification of Research Gaps

A critical analysis of the literature reveals a distinct research gap. While 3D TOM has been applied to grippers [1], its implementation with advanced nonlinear solvers like MMA, specifically tailored for the FDM/PLA process chain, remains underexplored. Many studies utilizing accessible manufacturing either compromise on structural performance or rely on 2D optimization, which introduces a disconnect between the optimized design and the final 3D product. There is a compelling need for an integrated methodology that leverages the full power of 3D optimization algorithms directly with low-cost AM to create grippers that are not only highly adaptive but also possess competitive payload capacity.

This study aims to bridge this gap by:

(1) Implementing a systematic 3D TOM framework using the SIMP method and the MMA solver to design monolithic compliant fingers that fully exploit the mechanical properties of PLA.

(2) Providing a direct comparative analysis of the MMA against a conventional solver (quadratic approximation) for a 3D compliant mechanism, highlighting convergence and performance differences.

(3) Developing and experimentally validating a series of low-cost, 3D-printed grippers, demonstrating that sophisticated optimization can yield performance competitive with commercial counterparts while maintaining the advantages of accessibility and low cost.

By doing so, this work establishes a robust reference for the effective use of MMA in 3D structural optimization and presents a viable pathway for the design of high-performance, economically accessible robotic end-effectors.

III. Methodology

This section details the systematic methodology employed for the development of the compliant robotic grippers. The process, illustrated in Fig. 1, encompassed a sequence of stages: (1) the implementation of the topology optimization theory and computational framework; (2) the optimization design of the flexible fingers; (3) the optimization design of the rigid support structures; (4) finite element validation of the optimized designs; and (5) the manufacturing and experimental testing of the final gripper prototypes.

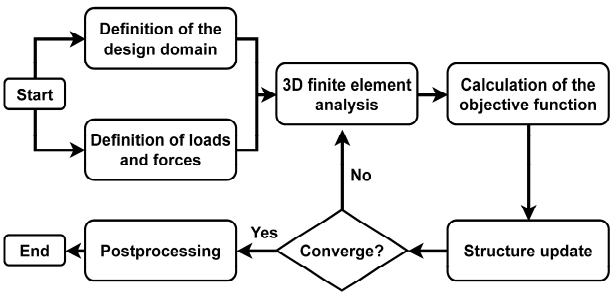

Fig. 1. Flowchart of the topological optimization procedure.

A. Topology Optimization Theory and Computational Implementation

1) TOM design concept

The TOM was employed to generate the conceptual layout for both the flexible fingers and the rigid support structures. Although the objective functions differed, the fundamental design procedure, summarized in Fig. 2, was consistent for both cases. The process begins by defining the design domain, applied loads, and support conditions. A Finite Element Analysis (FEA) is then performed to compute the objective function and its sensitivity to changes in each element's density. This information is used by an optimization algorithm to update the material density distribution across the design domain. This iterative loop continues until the objective function converges to an optimum, resulting in a voxel-based optimized structure. A final post-processing stage converts this result into a smooth, watertight geometry suitable for 3D printing.

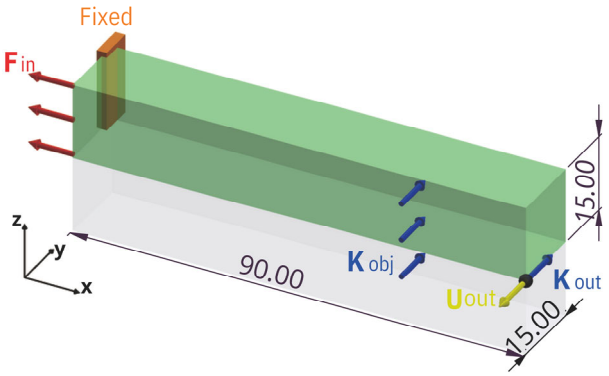

Fig. 2. Design domain for the topological optimization of the flexible finger.

2) Mathematical formulation

The optimization process was based on the SIMP method. SIMP assigns an optimal pseudo-density, $\tilde{x}_i$, to each finite element i within the discretized design domain, effectively determining the presence (1) or absence (0) of material. The relationship between the pseudo-density and the element's Young's modulus is given by Eq. (1):

$$E_i(\tilde{x}_i) = E_{min} + (\tilde{x}_i)^p (E_0 - E_{min}) \quad \tilde{x}_i \in [0,1] \tag{1}$$

where E_i is the interpolated Young's modulus of element i, E_0 is the modulus of the solid material, E_{min} is a very small modulus assigned to void regions to prevent numerical singularity, and p is the penalty factor p (typically $p = 3$) that encourages a solid-void solution.

The structural response under the applied loads is governed by the equilibrium Eq. (2):

$$K(\tilde{x})U(\tilde{x}) = F \tag{2}$$

where K is the global stiffness matrix, which is a function of the material distribution $\tilde{x}$, U is the global displacement vector, and F is the global force vector.

3) Computational algorithm

The TOM was implemented in MATLAB, building upon the open-source code "top3d" [16]. The core algorithm requires six input parameters: the number of elements in the x, y, and z directions $(nelx, nely, nelz)$, the volume fraction $(volfrac)$, the penalty factor $(penal)$, and a filter radius $(rmin)$ to control minimum feature size and ensure mesh-independence. The reference algorithm was significantly modified to incorporate the MMA [11] as the solver for the nonlinear optimization problem associated with the flexible finger design. A summary of the implemented algorithm is presented in Algorithm 1.

Algorithm 1 Flexible Mechanism Algorithm

1: Initialize input parameters and material properties
2: Define design domain and finite element mesh
3: **while** (change > tolerance) and (loop < max_iterations) **do**
4: Perform Finite Element Analysis (FEA)
5: Compute objective function and constraint
6: Perform sensitivity analysis
7: Update design variables using MMA
8: Apply density filter
9: Check for convergence
10: **end while**
11: Output optimized density distribution

B. Optimization Design of the Flexible Finger

1) Design domain and objective function

The design domain for the flexible finger is illustrated in Fig. 2. An input force F_{in} is applied to one end to actuate the mechanism. A output displacement U_{out} is generated at the opposite end, which serves as the gripping surface. A virtual spring with stiffness k_{obj} is included at the output port to model reaction from the object being grasped and to ensure the stability of the optimization process. The goal was to find the material distribution that maximizes U_{out}. This is formulated as the following optimization problem Eq. (3):

$$\begin{aligned} \text{Find} \quad & \tilde{x} = [x_1, x_2, x_3, \ldots\ldots, x_e, \ldots. x_n]^T \\ \text{Maximize} \quad & c(\tilde{x}) = -U_{out}(\tilde{x}) = -L^T U(\tilde{x}) \\ \text{Subject to} \quad & \frac{v(\tilde{x})}{v_0} - \bar{v} \leq 0 \\ & x \in X, X = x \in \mathbb{R}^n : 0 \leq X \leq 1 \end{aligned} \tag{3}$$

where L is a binary vector that selects the output displacement from the global displacement vector U, $v(\tilde{x})$ and v_0 are the current and full volume, respectively, and $\bar{v}$ is the prescribed volume fraction.

2) Implementation and solver comparison

The optimization was performed with the following parameters: nelx = 90, nely = 15, nelz = 15, volfrac = 0.10, penal = 3, rmin = 1.8.

To underscore the necessity of an advanced solver, the problem was first solved using a conventional quadratic approximation method [14]. As shown in Figs. 3 and 4, this method failed to converge after 200 iterations, producing a non-functional structure with poor structural clarity.

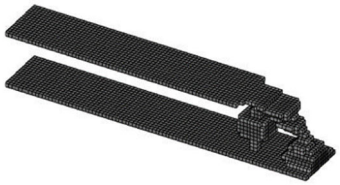

Fig. 3. Result of the optimization process using quadratic approximations for the flexible finger.

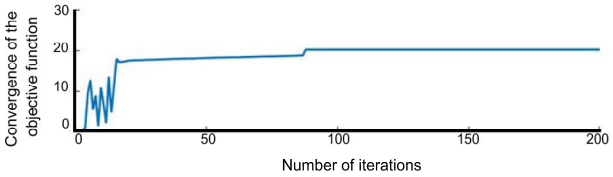

Fig. 4. Convergence of the flexible structure using quadratic approximations.

The problem was then solved using the MMA. The sub-problem solved at each iteration is given by Eq. (4):

$$\text{Maximize } C(\tilde{x}) + \sum_{i=1}^{m} \frac{\alpha_i}{v_i(\tilde{x})} \tag{4}$$

where $v_i(\tilde{x})$ are the constraint functions and α_i are adjustable parameters. The evolution of the design through the optimization process is shown in Fig. 5. leading to a clear and functional compliant mechanism (Fig. 6). The MMA achieved convergence at iteration 123, as illustrated in Fig. 7. Finally, the voxel-based model was post-processed using CAD software to obtain a smooth and manufacturable geometry, as shown in Fig. 8.

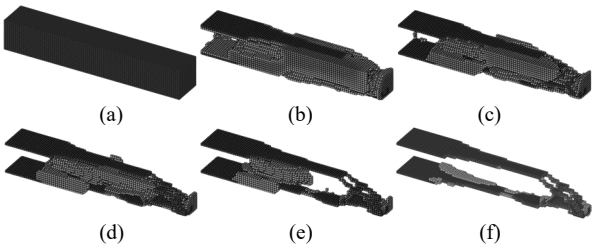

Fig. 5. Flexible finger optimization evolution process. (a) design domain; (b) iteration 25; (c) iteration 50; (d) iteration 75; (e) iteration 100; (f) iteration 123.

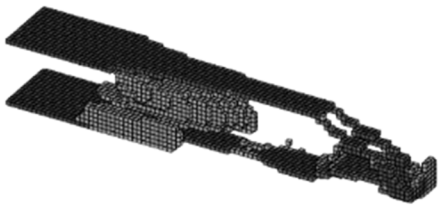

Fig. 6. Result of the optimization process using MMA for the flexible finger.

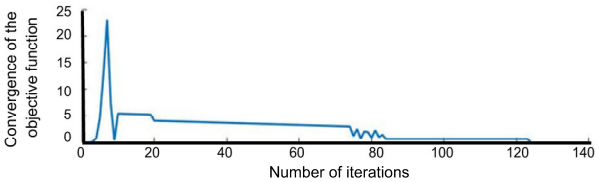

Fig. 7. Convergence of the flexible structure using MMA.

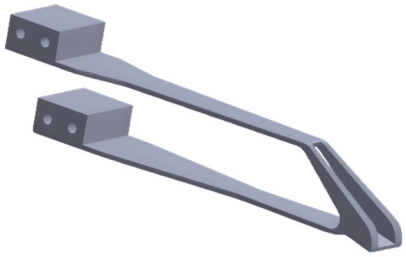

Fig. 8. Post-processing of the flexible structure.

C. Optimization Design of the Support Structures

1) Objective function for rigid structures

The support structures, which hold the flexible fingers and connect to the linear actuator, were optimized for maximum stiffness with a mass constraint. Unlike the flexible finger, the goal here was to minimize compliance (maximize stiffness). The optimization problem is formulated as Eq. (5):

$$\begin{aligned} \text{Find} \quad & \tilde{x} = [x_1, x_2, x_3, \ldots\ldots, x_e, \ldots. x_n]^T \\ \text{Maximize} \quad & c(\tilde{x}) = F^T U(\tilde{x}) \\ \text{Subject to a} \quad & v(\tilde{x}) = \tilde{x}^T V - \tilde{v} \leq 0 \\ x \in X, \quad & X = \{x \in \mathbb{R}^n \ : \ 0 \leq X \leq 1\} \end{aligned} \tag{5}$$

Given the relatively small displacements and linear nature of this stiffness-maximization problem, the computationally efficient quadratic approximation method was deemed sufficient and was used for these components.

2) Fixed structure optimization

The design domain for the fixed structure, which attaches to the stationary part of the actuator, is shown in Figs. 9 and 10. To reduce computational cost, symmetry was exploited by optimizing only one half of the domain. The complete structure was later mirrored in CAD. The optimization parameters were: nelx = 40, nely = 12, nelz = 120, volfrac = 0.40, penal = 3, rmin = 1.5.

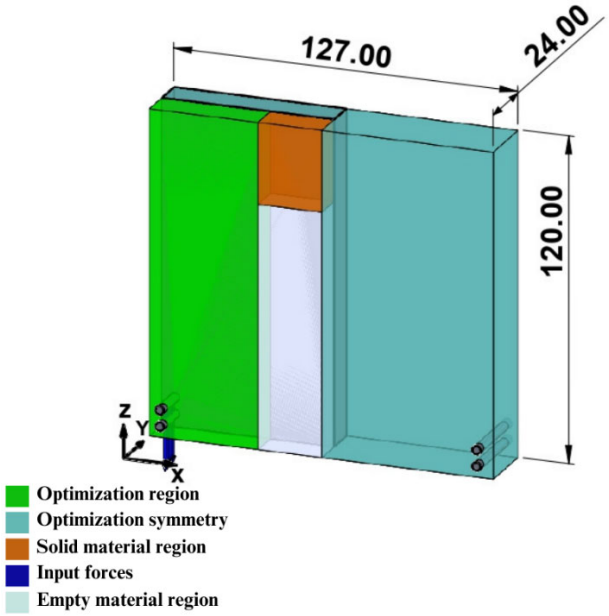

Fig. 9. Parameterization of the optimization region for the fixed structure.

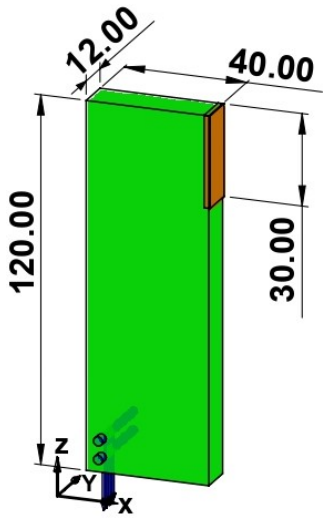

Fig. 10. Design domain for the topological optimization of the fixed structure.

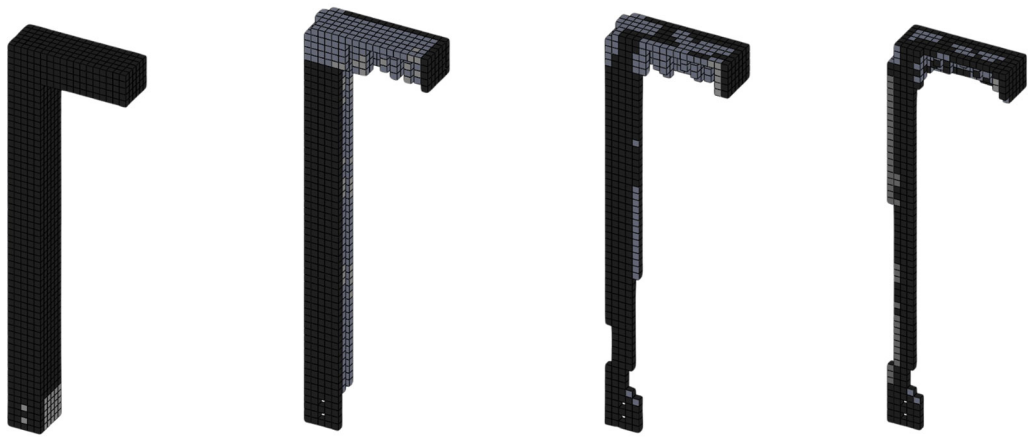

(a) (b) (c) (d)

Fig. 11. Fixed structure optimization evolution process. (a) design domain; (b) iteration 30; (c) iteration 60; (d) iteration 30.

The optimization evolution is shown in Fig. 11, with the final post-processed and mirrored structure presented in Fig. 12. The resulting design was adapted for the two-, three-, and four-finger grippers, as shown in Fig. 13.

3) Mobile structure

The mobile structure, which connects to the moving part of the actuator and pushes the fingers, was optimized similarly. The design domain is shown in Figs. 14 and 15. The parameters used were: nelx = 45, nely = 12, nelz = 12, volfrac = 0.40, penal = 3, rmin = 1.5.

The optimization process is depicted in Fig. 16, and the final structures for the different gripper configurations are shown in Figs. 17 and 18.

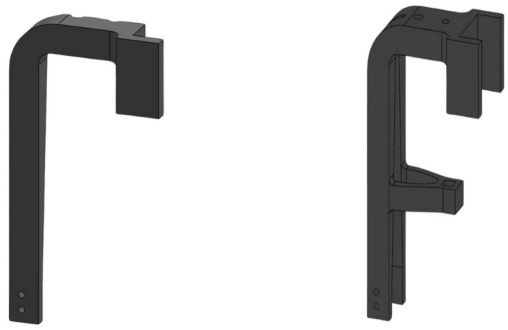

(a) (b)

Fig. 12. Optimized structure. (a) post-processing; (b) complete structure through design symmetry.

(a) (b) (c)

Fig. 13. Post-processing of the fixed structures designed. (a) two fingers; (b) three fingers; (c) four fingers.

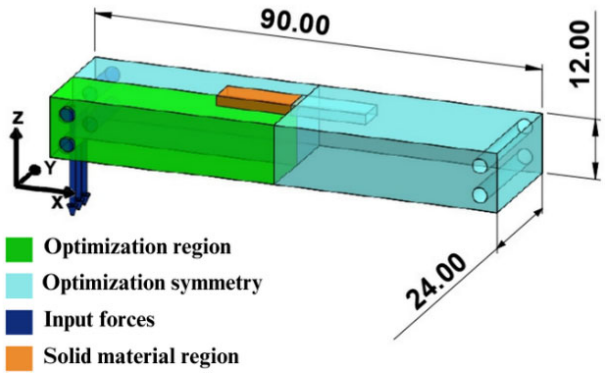

Fig. 14. Parameterization of the optimization region for the mobile structure.

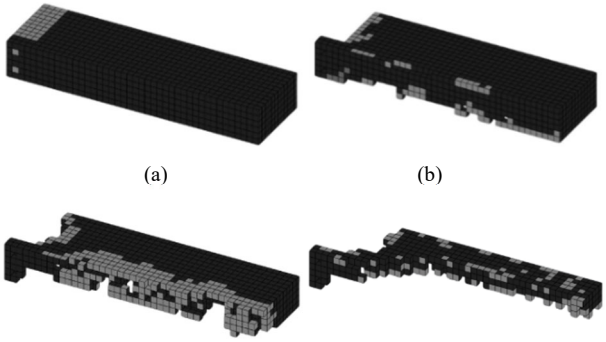

(a) (b) (c) (d)

Fig. 16. Fixed structure optimization evolution process. (a) design domain; (b) iteration 25; (c) iteration 50; (c) iteration 67.

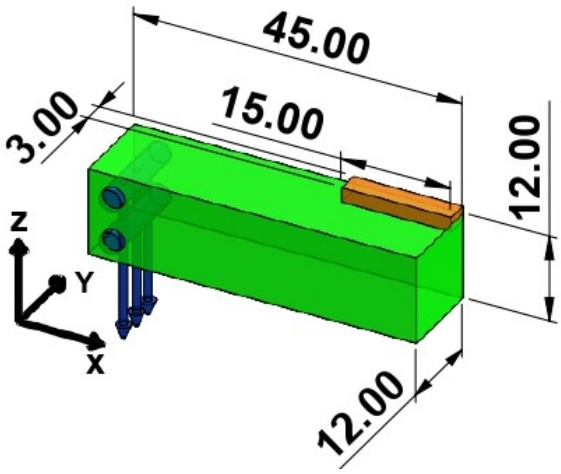

Fig. 15. Design domain for the topological optimization of the fixed structure.

(a) (b)

Fig. 17. Optimized structure. (a) post-processing; (b) complete structure through design symmetry.

(a) (b) (c)

Fig. 18. Post-processing of the mobile structures designed. (a) two fingers; (b) three fingers; (c) four fingers.

D. Finite Element Model for Validation

Prior to manufacturing, the performance of the optimized flexible fingers was validated through non-linear static FEA using Solidworks. The voxel-based optimized results were converted to a smooth CAD model and meshed with solid elements. The boundary conditions and load application mirrored those of the optimization design domain (Fig. 2). A static input force of 20 N, corresponding to the maximum force of the ECO-LLC linear motor, was applied.

The simulations compared the force-displacement relationship and stress distribution of the finger optimized by MMA versus the one from the quadratic approximation method. The results, shown in Figs. 19 and 20, confirmed the superior performance of the MMA-optimized design, which achieved a larger output displacement with lower stress concentrations under the same input force.

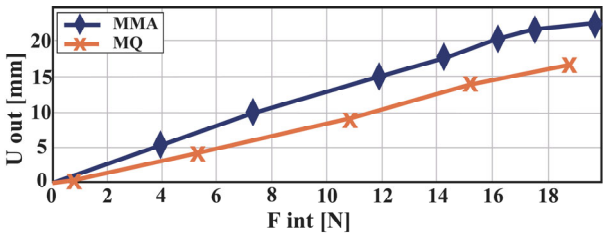

Fig. 19. Ratio between input force and output displacement of the flexible fingers optimized by Quadratic Approximation (MQ) and MMA.

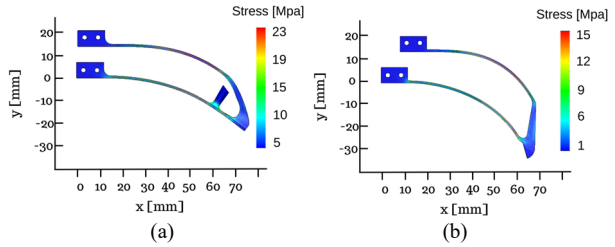

Fig. 20. Simulated deformation and stress distribution of flexible fingers with the same input force F_{int} = 20 N. (a). finger optimized by Quadratic approximations; (b) finger optimized by MMA.

E. Experimental Setup: Manufacturing and Validation

1) Manufacturing and assembly

All optimized parts, including the flexible fingers and support structures, were manufactured using FDM on a desktop 3D printer. PLA filament was used with standardized printing parameters (0.2 mm layer height, 60% infill density, 215°C nozzle temperature) to ensure consistency and mechanical reliability. The manufactured flexible finger is shown in Fig. 21. The components were assembled into two-, three-, and four-finger gripper configurations, as depicted in Fig. 22.

Fig. 21. Flexible finger manufactured by 3D printing.

Fig. 22. Parts manufactured by 3D printing. (a) two-finger gripper; (b) three-finger gripper; (c) four-finger grippe.

2) Experimental procedure

The assembled grippers were mounted on an ABB IRB-120 industrial robotic arm for testing, as shown for the three-finger configuration in Fig. 23. Two types of tests were conducted:

- Adaptability Tests: Ten objects with varied geometries, sizes, and surface characteristics (egg, ball, bottle, plush toy) were selected (Table I). The success of a stable grasp and lift for each object was recorded. The tests are illustrated in Figs. 24–26.
- Payload Tests: To determine the maximum load capacity, masses were gradually added to a container held by the gripper until failure occurred. The payload for each gripper configuration was recorded (Table II). The test setup is shown in Figs. 27–29.

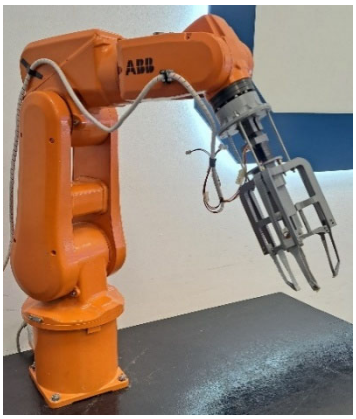

Fig. 23. Implementation of the three-finger gripper on the ABB IRB 120 robotic arm.

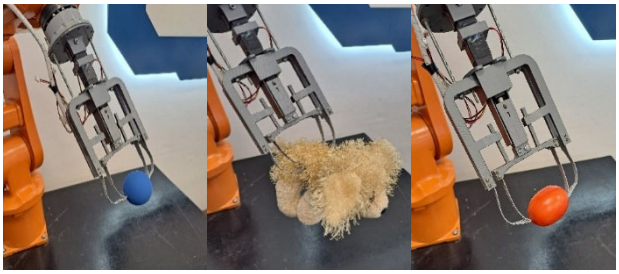

Fig. 24. Manipulation of different objects with the two-finger gripper: (a) Ball; (b) Plush toy; (c) Tomato.

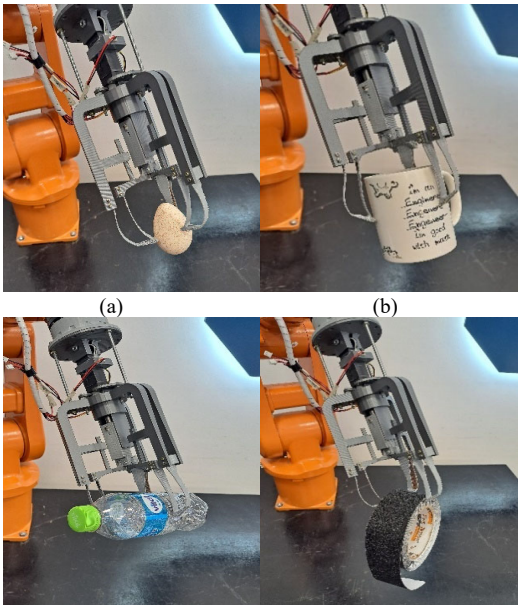

(a) (b) (c) (d)

Fig. 25. Manipulation of different objects with the three-finger gripper. (a) Egg; (b) Cup; (c) Bottle; (d) Scotch tape.

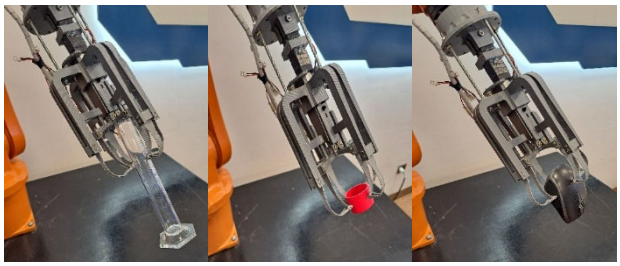

(a) (b) (c)

Fig. 26. Manipulation of different objects with the four-finger gripper. (a) Test tube; (b) Cylinder; (c) Mouse.

(a) (b)

Fig. 27. Two-finger gripper payload. (a) Manipulation; (b) manipulated mass.

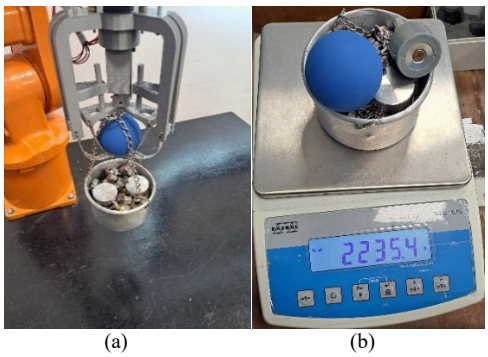

(a) (b)

Fig. 28. Three-finger gripper payload. (a) Manipulation; (b) manipulated mass.

(a) (b)

Fig. 29. Four-finger gripper payload. (a) Manipulation; (b) manipulated mass.

TABLE I. ADAPTABILITY RESULTS IN THE HANDLING OF DIFFERENT OBJECTS

Object	Two-Finger	Three-Finger	Four-Finger
Egg	Yes	Yes	Yes
Ball	Yes	Yes	Yes
Tomato	Yes	Yes	Yes
Mouse	Yes	Yes	Yes
Cup	Yes	Yes	Yes
Bottle	Yes	Yes	Yes
Test tube	Yes	Yes	Yes
Plush toy	Yes	Yes	Yes
Scotch Tape	Yes	Yes	Yes
Cylinder	Yes	Yes	Yes

TABLE II. OBJECT HANDLING PAYLOAD

Two-Finger (gr)	Three-Finger (gr)	Four-Finger (gr)
1507.8	2235.4	2774.7

IV. RESULTS AND DISCUSSION

This section presents the experimental validation of the topology-optimized grippers, evaluating their performance in terms of adaptability and payload capacity. The results are systematically analyzed, and the efficacy of the proposed MMA-based optimization methodology is discussed in the context of existing literature.

A. Experimental Validation of Optimized Designs

The finite element analysis and experimental tests were conducted to validate the performance of the designs generated by the Topology Optimization Method.

- Fig. 19 illustrates the force displacement relationship for the flexible fingers optimized using the MMA and the Quadratic Approximation method. The key phenomenon observed is that the MMA-optimized finger achieves a significantly larger output displacement for the same input force. This indicates a superior mechanical advantage, a direct result of the more efficient material distribution achieved by the MMA solver in navigating the nonlinear compliance problem.
- Fig. 20 provides a visual corroboration of this finding, displaying the simulated stress distribution and deformation under a 20 N input force. The finger optimized with quadratic

approximations (Fig. 20(a)) exhibits high-stress concentrations in localized, suboptimal hinges, leading to limited deformation. In contrast, the MMA-optimized finger (Fig. 20(b)) demonstrates a smoother, more distributed deformation with lower peak stresses, confirming the generation of a more effective and robust compliant mechanism.

- Fig. 21 presents the physical realization of the optimized design, confirming the manufacturability of the complex, organic geometry via FDM. The successful fabrication underscores the advantage of direct 3D topology optimization in producing readily printable structures without the need for manual interpretation from 2D results.

B. Gripper Performance Evaluation

The assembled two, three, and four finger grippers were subjected to rigorous adaptability and payload testing.

1) Adaptability performance

The results of the adaptability tests are summarized in Table I. The grippers successfully manipulated all ten objects, which encompassed a wide range of geometries (spherical, cylindrical, irregular), sizes, and surface textures (smooth, compliant). Figs. 24–26 visually document the successful grasping of representative objects, including fragile items like an egg and a tomato, and irregular shapes like a plush toy. The 100% success rate across all configurations demonstrates the exceptional adaptive capability inherent to the compliant mechanism design. This adaptability stems from the passive conformity of the monolithic fingers, which distribute contact forces evenly, thereby securing objects without requiring complex sensor feedback or control algorithms.

2) Payload capacity analysis

The quantitative payload capacity of each gripper configuration is reported in Table II. The maximum loads were recorded as 1.51 kg, 2.24 kg, and 2.77 kg for the two-, three-, and four-finger grippers, respectively. Figs. 27–29 depict the experimental setup for these tests. The positive correlation between the number of fingers and the payload capacity is attributed to the increased number of contact points and the consequent distribution of the load's moment over a larger structural area. This trend validates the structural integrity of the optimized support structures, which were designed for maximum stiffness under a mass constraint.

C. Comparative Analysis with Existing Literature

The performance of the proposed grippers is contextualized by comparing key metrics with those reported in recent and relevant studies, as summarized in Table III.

TABLE III. COMPARATIVE ANALYSIS WITH EXISTING GRIPPER SYSTEMS

Gripper System	Manufacturing Method/Material	Optimization Approach	Max. Payload	Key Features/Limitations
This Work (Four-Finger)	FDM/PLA	3D TOM (SIMP/MMA)	2.77 kg	Low-cost, high adaptability, competitive payload for material
LARG Gripper [1]	SLS/Nylon	3D TOM	8.3 kg	High payload but high manufacturing cost
Hello Robot Stretch [23]	Not Specified/Not Specified	Not Specified	~2.0 kg	Commercial benchmark, higher unit cost
Source Robotics SSG-48 [24]	Not Specified/Not Specified	SLS/Nylon	~3.0 kg	Commercial benchmark, higher unit cost
Petkovic and Pavlovic [3]	Conventional/Not Specified	FDM/PLA	Not Specified	Early compliant design; lower reported performance

1) Payload capacity

The payload of 2.77 kg for the four-finger gripper is highly competitive. It surpasses the capacity of commercial systems like the Hello Robot Stretch gripper (~2 kg) [23] and approaches that of the Source Robotics SSG-48 (~3 kg) [24]. More significantly, it achieves this while being fabricated via low-cost FDM with PLA, unlike the study by Sun *et al.* [1], which achieved a higher payload (8.3 kg) but relied on high-end SLS with advanced polymers, resulting in substantially higher manufacturing costs. This comparison highlights the core contribution of this work: the application of advanced 3D optimization (MMA) enables the extraction of high performance from a low-cost material and process chain.

2) Adaptability and design methodology

The demonstrated adaptability is consistent with the advantages of compliant mechanisms cited in the Refs. [1, 3]. However, this study advances the field by systematically deriving the compliant geometry through a 3D optimization process. Many prior works relying on FDM/PLA either used 2D optimization [5, 8], which requires manual interpretation and can compromise performance, or employed simpler optimization schemes that failed to converge to a functional design, as evidenced by our own comparative solver analysis (Figs. 3 and 4). The successful manipulation of fragile objects validates that the MMA-optimized fingers generate sufficient displacement with low, non-damaging contact forces.

3) Computational efficiency

The superiority of the MMA solver, a key focus of this study, is unequivocally demonstrated. The MMA achieved convergence in 123 iterations (2 h 15 min), whereas the conventional quadratic approximation method failed to converge even after 200 iterations (5 h 25 min). This represents not only a 58% reduction in computational time but, more importantly, the successful synthesis of a functional mechanism versus a non-functional one. This

finding aligns with the theoretical advantages of MMA for handling nonlinear constraints [11, 12] and provides a valuable reference for future implementations in 3D compliant mechanism synthesis.

In summary, the experimental results confirm that the proposed methodology, centered on MMA-based 3D topology optimization, provides an effective framework for developing high-performance, low-cost compliant robotic grippers. The grippers bridge a critical gap in the literature by demonstrating that sophisticated computational design can unlock performance from accessible manufacturing methods that is competitive with both commercial products and research prototypes employing more expensive solutions.

V. Conclusions

This research successfully implemented a systematic topology optimization methodology based on the SIMP approach combined with the MMA algorithm for the development of cost-effective robotic grippers with flexible fingers. The results demonstrate that the MMA method outperforms quadratic approximation techniques, achieving convergence in 123 iterations with a computational time of 2 h 15 min, whereas quadratic approximations required more than 5 h 25 min without reaching convergence. This represents a 58% reduction in computational time while ensuring an optimal distribution of material within the flexible fingers.

Experimental validation confirmed the effectiveness of the optimized designs, achieving payload capacities of 1.5 kg, 2.2 kg, and 2.7 kg for the two-, three-, and four-finger grippers, respectively. These results are comparable to those of commercial solutions such as Hello Robot (2 kg) and approach the performance of Source Robotics grippers (3 kg), while significantly reducing manufacturing costs through the use of additive manufacturing with PLA material.

Furthermore, the grippers demonstrated robust manipulation capabilities across a wide range of objects, including fragile items such as eggs and tomatoes, as well as irregularly shaped objects like plush toys. A 100% success rate was achieved across all tested geometries, highlighting the adaptability and effectiveness of the compliant mechanisms. Additionally, the MMA-optimized fingers required lower actuation forces to achieve equivalent displacements when compared to designs obtained through quadratic approximation methods, indicating improved internal material distribution and enhanced mechanical efficiency.

Conflict of Interest

The authors declare no conflict of interest.

Author Contributions

BL conducted the research and wrote the manuscript; JB contributed to the translation and experimental validation; BQ supervised the research; all authors had approved the final version.

References

[1] Y. Sun, Y. Liu, F. Pancheri *et al.,* "LARG: A lightweight robotic gripper with 3-D topology optimized adaptive fingers," *IEEE/ASME Transactions on Mechatronics*, vol. 27, no. 4, pp. 2026–2034, 2022.

[2] L. L. Howell, "Compliant mechanisms," in *21st Century Kinematics,* J. McCarthy, Ed. London, U.K.: Springer, 2013, pp. 189–215. doi: 10.1007/978-1-4471-4510-3_7

[3] D. Petkovic and N. D. Pavlovic, "Compliant multi-fingered passively adaptive robotic gripper," *Multidiscipline Modeling in Materials and Structures*, vol. 9, no. 4, pp. 538–547, 2013.

[4] S. Liao, B. Ding, and Y. Li, "Design, assembly, and simulation of flexure-based modular micro-positioning stages," *Machines*, vol. 10, no. 6, 421, 2022.

[5] Q. Wang, H. Han, C. Wang *et al.,* "Topological control for 2D minimum compliance topology optimization using SIMP method," *Structural and Multidisciplinary Optimization*, vol. 65, no. 1, 2022.

[6] C.-H. Liu, F.-M. Chung, and Y.-P. Ho, "Topology optimization for design of a 3D-printed constant-force compliant finger," *IEEE/ASME Transactions on Mechatronics*, vol. 26, no. 4, pp. 1828–1836, 2021.

[7] N. Lobontiu, *Compliant Mechanisms: Design of Flexure Hinges*, 1st ed. Boca Raton, USA: CRC Press, 2022.

[8] C.-H. Liu, C.-H. Chiu, M.-C. Hsu *et al.,* "Topology and size–shape optimization of an adaptive compliant gripper with high mechanical advantage for grasping irregular objects," *Robotica*, vol. 37, no. 8, pp. 1383–1400, 2019.

[9] M. P. Bendsøe and O. Sigmund, "Material interpolation schemes in topology optimization," *Archive of Applied Mechanics*, vol. 69, no. 9–10, pp. 635–654, 1999.

[10] M. Zhou and G. I. N. Rozvany, "The COC algorithm, Part II: Topological, geometrical and generalized shape optimization," *Computer Methods in Applied Mechanics and Engineering*, vol. 89, no. 1–3, pp. 309–336, 1991.

[11] K. Svanberg, "The method of moving asymptotes—a new method for structural optimization," *International Journal for Numerical Methods in Engineering*, vol. 24, no. 2, pp. 359–373, 1987.

[12] D. Jung and H. C. Gea, "Topology optimization of nonlinear structures," *Finite Elements in Analysis and Design*, vol. 40, no. 11, pp. 1417–1427, 2003.

[13] O. Sigmund, "On the design of compliant mechanisms using topology optimization," *Journal of Structural Mechanics*, vol. 25, no. 4, pp. 493–524, 1997.

[14] L. Li and K. Khandelwal, "An adaptive quadratic approximation for structural and topology optimization," *Computers & Structures*, vol. 151, pp. 130–147, 2015.

[15] K. Svanberg. (2014). MMA and GCMMA-two methods for nonlinear optimization. *Semantic Scholar*. [Online]. Available: https://api.semanticscholar.org/CorpusID:211105912

[16] K. Liu and A. Tovar, "An efficient 3D topology optimization code written in Matlab," *Structural and Multidisciplinary Optimization*, vol. 50, no. 6, pp. 1175–1196, 2014.

[17] C.-H. Liu, Y. Chen, and S.-Y. Yang, "Topology optimization and prototype of a Multimaterial-Like compliant finger by varying the infill density in 3D printing," *Soft Robotics*, vol. 9, no. 5, pp. 837–849, 2021.

[18] T. Letcher and M. Waytashek, "Material property testing of 3D-Printed specimen in PLA on an entry-level 3D printer," in *Proc. the ASME 2014 International Mechanical Engineering Congress & Exposition, Volume 2A: Advanced Manufacturing*, 2014.

[19] A. R. Torrado, C. M. Shemelya, J. D. English *et al.,* "Characterizing the effect of additives to ABS on the mechanical property anisotropy of specimens fabricated by material extrusion 3D printing," *Additive Manufacturing*, vol. 6, pp. 16–29, 2015.

[20] W. Gao, Y. Zhang, D. Ramanujan *et al.*, "The status, challenges, and future of additive manufacturing in engineering," *Computer-Aided Design*, vol. 69, pp. 65–89, 2015.

[21] F. Chen, W. Xu, H. Zhang *et al.*, "Topology optimized design, fabrication, and characterization of a soft cable-driven gripper," *IEEE Robotics and Automation Letters*, vol. 3, no. 3, pp. 2463–2470, 2018.

[22] D. Yago, J. Cante, O. Lloberas-Valls *et al.*, "Topology optimization methods for 3D structural problems: A comparative study," *Archives of Computational Methods in Engineering*, vol. 29, no. 3, pp. 1525–1567, 2021.

[23] Stretch open-source mobile manipulator. *Hello Robot*. [Online]. Available: https://hello-robot.com/stretch-3-product

[24] Source Robotics. (Dec 2025). Source robotics | Open source robotic arms - PAROL6. *Source Robotics*. [Online]. Available: https://source-robotics.com/?srsltid=AfmBOoqCYtlMqQYB9mL2uUM_tW0LDAoWLBh3A7BOgKlr__C4AD42828H